CXCR4 allows T cell acute lymphoblastic leukemia to escape from JAK1/2 and BCL2 inhibition through CNS infiltration.

Short Title: JAK1/2-BCL2-CXCR4 inhibition for T-ALL treatment

Kirsti L. Walker,[1] Sabrina A. Kabakov,[1] Fen Zhu,[3] Myriam N. Bouchlaka,[1] Sydney L Olson,[1] Monica M. Cho,[1] Aicha E. Quamine,[1] Arika S. Feils,[1] Tara B. Gavcovich,[1] Lixin Rui,[2,3] and Christian M. Capitini [1, 2]

[1] Department of Pediatrics, University of Wisconsin School of Medicine and Public Health, 1111 Highland Avenue, Madison, WI 53705 USA
[2] Carbone Cancer Center, University of Wisconsin School of Medicine and Public Health, 1111 Highland Avenue, Madison, WI 53705 USA
[3] Department of Medicine, University of Wisconsin School of Medicine and Public Health, 1111 Highland Avenue, Madison, WI 53705 USA

Corresponding authors:

Lixin Rui - lrui@medicine.wisc.edu

Christian Capitini - ccapitini@pediatrics.wisc.edu, T: (608)262-2415, F: (608)265-9721

Text word count: 3,994 words
Abstract word count: 226 words
# of figures and tables: 6
# of references: 42

Key Points

- Ruxolitinib & venetoclax treat T-ALL *in vitro*; fail to treat CNS burden *in vivo*.

- CXCR4-CXCL12 recruits T-ALL to CNS and accelerates lethality.

Abstract

Relapsed/refractory T cell acute lymphoblastic leukemia (T-ALL) is difficult to salvage especially in heavily pretreated patients, thus novel targeted agents are sorely needed. Hyperactivated JAK/STAT and BCL2 overexpression promote increased T-ALL proliferation and survival, and targeting these pathways with small molecule inhibitors like ruxolitinib and venetoclax may provide an alternative therapeutic approach to re-induce clinical remissions. Ruxolitinib and venetoclax show a dose-dependent effect individually, but combination treatment synergistically reduces survival and proliferation of Jurkat and Loucy cells *in vitro*. Using a xenograft CXCR4+ Jurkat model, the combination of ruxolitinib and venetoclax fails to improve survival, with the primary cause of death from hind limb paralysis. Despite on-target inhibition of the drugs on total STAT1, pSTAT1, total STAT3, total STAT5 and pSTAT5 as well as BCL2, histopathologic analysis demonstrates increased leukemic infiltration into the central nervous system (CNS), which expresses CXCL12, as compared to the liver or bone marrow. Liquid chromatography-tandem mass spectroscopy shows that neither ruxolitinib nor venetoclax can effectively cross the blood-brain barrier, limiting efficacy against CNS T-ALL. Deletion of CXCR4 on Jurkat cells by CRISPR/Cas9 results in prolonged survival and a reduction in overall and neurologic clinical scores. While combination therapy with ruxolitinib and venetoclax shows promise for treating T-ALL, additional inhibition of the CXCR4-CXCL12 axis will be needed to eliminate both systemic and CNS T-ALL burden and maximize the possibility of complete remission.

Introduction

T cell acute lymphoblastic leukemia (T-ALL) occurs when mutated thymocytes that are destined for cell death survive and acquire additional mutations that promote full malignant transformation.[1] Cure rates, respectively, reach 60% in adults and over 80% in pediatric patients when treated with combination chemotherapy protocols.[2-4] However, resistance to first-line therapy is seen in 25% of children and more than 50% of adults, and the cohort that do respond to current ALL chemotherapy protocols often suffer from both acute and chronic toxic side-effects despite treatment success.[5] Therefore, there is a need for the development of novel, non-chemotherapeutic treatments for T-ALL.[6,7]

In order to improve prognosis and mitigate side-effects seen with current chemotherapy treatments, it is crucial to evaluate the underlying molecular pathways that drive T-ALL and contribute to chemotherapy resistance. Over the last decade, the Janus Activating Kinase/ Signal Transducer and Activator of Transcription (JAK/STAT) pathway has emerged as playing a critical pathogenic role in several hematologic malignancies including T-ALL.[8,9] Activation of JAK tyrosine kinases leads to the subsequent phosphorylation and activation of STAT transcription factors. Specifically, JAK1 or TYK2 are known to activate and phosphorylate STAT1 (pSTAT1), which is constitutively activated in leukemias and lymphomas.[10-12] Sanda et al 2013 demonstrated that many T-ALL cases are dependent upon the TYK2-STAT1-BCL2 pathway[1]. BCL2 is an anti-apoptotic protein that is pathologically overexpressed in several cancer types to increase survival[13-15], including T-ALL.[16] These pathways allow for increased T-ALL proliferation through the JAK/STAT pathway and increased T-ALL survival through increased BCL2 expression.

Ruxolitinib is an FDA approved small molecule inhibitor that targets JAK1 and JAK2. Ruxolitinib prevents the tyrosine phosphorylation of STAT1/3/5, which are downstream of cytokine receptors that drive T-ALL proliferation (e.g. IL-7), and should function to inhibit the

proliferative properties seen in T-ALL. Unfortunately for most patients, chronic therapy with ruxolitinib results in reactivation of JAK/STAT signaling and prevents T-ALL remission.[17] In these cases, BCL2 may also be hijacked and upregulated to promote survival of these cancer cells.[1]

Venetoclax is a highly potent and specific BH3 mimitec which binds to the BCL2 protein without targeting platelets. This causes the downregulation of BCL2 and the eventual cell death of T-ALL.[16,18,19] The combination of ruxolitinib and venetoclax is emerging as a viable treatment option for relapsed disease. These drugs were previously utilized to treat IL-7 receptor alpha (IL7Rα)-mutated T-ALL, which prolonged survival in a preclinical model but ultimately all animals succumbed to leukemia.[20] Because the central nervous system (CNS) is a common site of T-ALL involvement,[2,21] one potential limitation of inhibiting these pathways *in vivo* is that it is unknown if these drugs can cross the blood-brain barrier (BBB). Also, the mechanism by which T-ALL would escape the combination of ruxolitinib and venetoclax is entirely unknown.

This study demonstrates that ruxolitinib and venetoclax work synergistically *in vitro* to treat T-ALL, but are not effective *in vivo* by showing for the first time the inability of these drugs to effectively cross the BBB and treat T-ALL in the CNS. CXCR4-CXCL12 has been implicated as a potential pathway that drives T-ALL infiltration into the CNS.[22-25] By deleting the CXCR4 gene from T-ALL, we confirm previous findings that demonstrate prolonged survival *in vivo* with decreased overall and neurologic clinical scores.[22,23] Thus, in the setting of CXCR4 inhibition, T-ALL CNS infiltration would be blocked and potentially ruxolitinib and venetoclax may be able to clear systemic disease.

Methods

Tumor cell lines

Jurkat (TIB-152) clone E6-1 and Loucy (CRL-2629) (ATCC Manassas, VA) were used as human T-ALL cell lines. Jurkat-GFP cell line was generated by transfecting $2x10^5$ Jurkat cells using the Lonza 4D-Nucleofector X Unit (Basel, Switzerland). Nucleofector was used to deliver 1 µg of px330 plasmid encoding for Cas9 protein and a gRNA for the AAVS1 locus and 1 µg of an AAVS1-CAGGS-EGFP plasmid to serve as donor template. Nucleofection was carried out in SE buffer using a CL-120 pulse code for transfection. Cells were cultured in RPMI post-nucleofection and sorted on a FACSAria for GFP+ cells. Cells were cultured in RPMI 1640 1x medium supplemented with 10% heat-inactivated FBS (Gemini bio-products, Sacramento, CA), L-Glutamine (2 mM), penicillin/streptomycin (100 µ/ml) at 37°C, 5% CO_2 and 95% humidity. Excluding FBS, all other media ingredients were purchased from Corning, Corning, NY. All cell lines were mycoplasma tested and authenticated prior to use (IDEXX Bioresearch, Westbrook, ME).

In vivo T-ALL xenograft model

NOD/SCID/*Il2rg*^{tmwjl}/Szj (NSG) breeder mice were purchased from Jackson Labs (Bar Harbor, ME) and bred internally at the UW Madison Mouse Breeding Core and Services (BRMS), Madison, WI. Mice were housed in accordance with the Guide for the Care and Use of Laboratory Mice and experiments were performed under an animal protocol approved by the institutional animal care and use committee. Both male and female mice aged 8- 16 weeks were randomized into control or treatment groups. On Day +0, $2x10^6$ Jurkat cells in 200 µl of 1x PBS were injected intravenously into NSG mice to generate a xenograft T-ALL mouse model. Using flow cytometric analysis, at least 1% anti-human CD45 cancer burden was documented in the peripheral blood (usually day 5-7) before initiating treatments. Mice were orally gavaged once daily for 14-days with vehicle(s), 100µl 30 mg/kg/day ruxolitinib, 100µl 35 mg/kg/day venetoclax, or combination. Mice were monitored for survival, % weight change, and clinical symptoms of

disease (activity, hunch, and hind-limb paralysis) using a modified scoring system

(Supplementary Table 1).

Ruxolitinib and venetoclax treatments

Ruxolitinib (INCB018424) and venetoclax (ABT-199) were purchased in powdered form (Active

Biochemicals, Kowloon Bay, Kowloon, Hong Kong, Cat # A-1134, A-1231). *In vitro* use,

ruxolitinib was resuspended in 100% DMSO at a concentration of 100 mg/ml and diluted to a

working stock of 50 µM (final concentration of DMSO being 10%). *In vivo* use, ruxolitinib in

100% DMSO was added to 5% N,N-dimethylacetamide (Cat # D137510-500ml, Sigma Aldrich,

St. Louis, MO) + 0.5% methylcellulose (Cat # ME136, Spectrum Chemical, New Brunswick, NJ)

in H_2O. *In vitro* use venetoclax was resuspended in 100% warm DMSO at a concentration of 50

mg/ml and diluted to a working stock of 200 nM (final concentration of DMSO being 11%). *In*

vivo use venetoclax was resuspended in 100% EtOH at a concentration of 100 mg/ml.

Appropriate amount of venetoclax was resuspended in 10% -100% EtOH + 30% PEG 400 (Cat

1008415, Rigaku, The Woodlands, TX) + 60% Phosal 50 (Lipoid, Ludwigshafen, Germany).

CRISPR-Cas9 deletion of CXCR4 in T-ALL

Jurkat cells were cultured in usual media supplemented with 25 ng/mL Amphotericin B (ATCC).

RNP delivery occurred via Electroporation. All CRISPR reagents were purchased from IDT,

Coralville, IA. RNP complex was prepared immediately before electroporation. $2x10^5$ cells were

used for each electroporation. CXCR4 exon 2 CRISPR RNA (crRNA)

(TACACCGAGGAAATGGGCTCAGG) and Atto-trans-activating crRNA (Atto-tracrRNA) were

mixed in equimolar concentrations (200 µM) to form a ctRNA::tracrRNA complex (ctRNA). The

molar ratio ctRNA to Cas9 was 1:1 with the working concentration of the electroporation being 2

µM Cas9:ctRNA and 2 µM Alt-R Cas9 electroporation enhancer. RNP was delivered into cells

using a Lonza (Basil, Switzerland) 4D-X Nucleofector according to manufacturer's specifications. Single cell sorting occurred 40 h after electroporation. Cells were harvested, washed, and treated with APC anti-human CXCR4 antibody (Cat #306509, Biolegend, San Diego, CA) and DAPI in accordance with the manufacturer's specifications. Cells were then sorted for APC·Atto· population on a BD FACSAria (BD Biosciences, Franklin Lakes, NJ) and placed into 1:1 conditioned growth media (fresh media: filtered media from fully confluent flask) for clonal outgrowth. Surviving clones were genotyped via amplicon sequencing on the MiSeq. The targeted region from each was then amplified via PCR, barcoded with a second PCR reaction, pooled, and run on a MiSeq Nano (University of Wisconsin Biotechnology Center, Madison, WI). Data analysis was performed with CRISPResso (PMID: 27404874). Selected clones carried compound heterozygous nonsense mutations in the targeted region.

Western blot analysis

Cells were collected and lysed using MAPK lysis buffer (4 mM sodium pyrophosphate, 50 mM HEPES, 100 mM NaCl, 1 mM EDTA, 10 mM NaF, 2 mM orthovanadate, pH 7.5) with protease inhibitor cocktail (Cat # P8340, Sigma Aldrich, St. Louis, MO; ThermoFisher, Waltham, MA) Protein concentrations were determined by BCA Assay (Cat # 23250, Thermo Fisher, Waltham, MA). Proteins were separated by SDS-PAGE and transferred to a nitrocellulose membrane. Membrane was blocked for 30 min with 5% non-fat milk in TBST at 20 °C, and incubated overnight at 4 °C with the following antibodies from Cell Signaling Technology, Danvers, MA unless otherwise stated: STAT1 (Cat #9172L), pSTAT1 (Cat #7649S), STAT3 (Cat # 124H6), pSTAT3 (Tyr705), (Cat #9145), STAT5 (Cat #25656S), pSTAT5 (Cat #9314S), BCL2 (Santa Cruz Biotechnology, sc7382), BIM (Cat #2933S), BAX (Cat #2774S), BAK (Cat #121058), Cytochrome C (Cat # 11940S), H3 (abcam, ab1791), β-Actin (Cat #4967), and CXCL12 antibody (Cat #3740). Membranes were then incubated for 1 h with 1:5000 anti-rabbit (Cat#

#7074) or anti-mouse (Cat #7076) HRP- conjugated secondary and developed using the

chemiluminescence HRP substrate kit (Cat # 34080, 34095, Thermo Fisher, Waltham, MA)

Liquid chromatography and tandem mass spectrometry

Analyses of ruxolitinib and venetoclax in organs were carried out on the LC/MS/MS Linear Ion

Trap Quadrupole system consisting of an Agilent 1100 High Pressure Liquid Chromatograph

(Santa Clara, CA) placed on the front end of an Applied Biosystems 3200 Q-Trap Mass

Spectrometer equipped with a Turbo V™ (Beverly Hills, CA) spray source running in the

Multiple Reaction Monitoring mode. Chromatography separated using Agilent ZORBAX SB-C18

Rapid Resolution HT reversed-phase column 2.1x 50 mm (1.8 µm particle size) onto which 1 µl

of methanol extracted sample was automatically loaded. HPLC delivered solvents A: 0.1% (v/v)

formic acid in water, and B: 0.1% formic acid in acetonitrile at 0.2 ml/min. After 2 min loading

and equilibration at 95% buffer A, analytes were eluted from the column directly into

electrospray orifice over 23 min 5% (v/v) B to 100% (v/v) B fast gradient, followed by a 5 min

hold at 100% (v/v) B and 9 min post gradient equilibration at 95% buffer A. As analytes eluted

from HPLC-column into electrospray source MRM mode selectively measured six transitions

based on precursor mass and specific fragment mass for drugs of interest. Transitions

measured were: m/z= 306.4, fragment m/z= 186.1 for most abundant MS/MS fragment of

ruxolitinib; m/z= 306.4, fragment m/z= 159.0 for second most abundant MS/MS fragment of

ruxolitinib; m/z= 435.0, fragment m/z= 321.1 for most abundant MS/MS fragment of doubly

charged $[M+2H]^{2+}$ venetoclax; m/z= 435.0, fragment m/z= 163.4 for second most abundant

MS/MS fragment of doubly charged $[M+2H]^{2+}$ venetoclax; m/z= 868.5, fragment m/z= 321.2 for

most abundant MS/MS fragment of singly charged $[M+H]^{+}$ venetoclax and m/z= 868.5, fragment

m/z= 233.1 for second most abundant MS/MS fragment of singly charged $[M+H]^{+}$ venetoclax.

The following instrumental parameters generated the most optimum protonated ions and

selectively diagnostic fragment ions: Ion spray voltage (IS), 4500 V; Curtain gas (CUR), 25 psi;

Nebulizer gas (GS1), 50 psi; Turbo gas (GS2), 30 psi; Turbo gas temperature (TEM), 650 °C;

Interface heather (ihe), ON; Collision Gas (CAD), Medium; Declustering potential (DP), 50 eV;

Entrance potential (EP), 10 eV; Collision energy (CE), 40 eV; Collision cell exit potential (CXP),

5 eV; Detector (CEM), 2500; Dwell time, 200 msec with pause time, 5 msec.

Statistical methods

GraphPad Prism version 7.0 for the Macintosh OS (GraphPad Software, San Diego, CA)

generated all statistics. Data were expressed as mean ± SEM. For analysis of 3 > groups, a

non-parametric ANOVA test was performed with the Bonferroni or Sidak's multiple comparisons

post-test. Analysis of differences between two normally distributed test groups was performed

using a two-sided Mann Whitney test. A p-value less than 0.05 was considered statistically

significant.

Data Sharing Statement

For original data, please contact ccapitini@pediatrics.wisc.edu

Results

Dysregulation of JAK/STAT and BCL2 in T-ALL patient samples

Secondary analysis of gene expression data from 14 different T-ALL patient samples

showed that JAK1/2, STAT1/3/5 gene expression were increased as compared to normal tissue

(NCI Oncogenomics St. Jude Leukemia Affy U133AB DB, https://pob.abcc.ncifcrf.gov/cgi-

bin/JK). While JAK1 and STAT1 showed evidence of increased and decreased gene expression

depending on the patient sample, JAK2 was consistently 1 to 2 standard deviations lower in

expression while STAT3/5 were 1 to 2 standard deviations higher in expression as compared to controls. Furthermore, BCL2 expression was 2 to 3 standard deviations higher than normal tissue controls. **(Figure 1A)**

Dosing of ruxolitinib or venetoclax alone decrease the survival and proliferation of T-ALL cells *in vitro*

To investigate the relevance of the JAK/STAT and BCL2 pathways on T-ALL proliferation and cell survival, Jurkat (mature T-ALL) and Loucy (early precursor T-ALL with high BCL2 expression) were assessed following treatment with either ruxolitinib or venetoclax.[15,26] These cell lines were treated with a serial dose of ruxolitinib and venetoclax over the course of 72 h and evaluated using a trypan blue exclusion assay and MTT proliferation assay. Ruxolitinib and venetoclax were able to decrease the survival and proliferation of both Jurkat **(Figure 1B-E)** and Loucy **(Supplementary Figure 1)** cell lines after 24, 48, and 72 h of treatment. At concentrations of 2.5 μM ruxolitinib **(Figure 1B)** or 0.05 μM venetoclax **(Figure 1C)**, the survival of the cell lines was statistically significantly reduced ($p < 0.005$). Further increased concentration of ruxolitinib to 5 μM resulted in statistically significant decreased cell survival ($p < 0.001$) compared to DMSO control **(Figure 1B)**. Similarly, the two highest doses of ruxolitinib (5 μM and 2.5 μM) and of venetoclax (0.5 μM and. 0.25 μM) also significantly lowered proliferation ($p < 0.0001$) compared to the DMSO control **(Figure 1D, E)**.

Ruxolitinib and venetoclax synergistically decrease survival and proliferation of T-ALL cells *in vitro*

After determining that ruxolitinib and venetoclax individually affect survival and proliferation of T-ALL, T-ALL cells were treated with ruxolitinib and venetoclax in combination and evaluated again for survival and proliferation. A synergistic dose was determined by Compusyn software **(Figure 2D)**. This synergistic dose was then tested for survival and proliferation in comparison to single-dose and DMSO controls in both cell lines **(Figure 2A, B, D; Supplementary Figure 2A, B)**. The synergistic effect of ruxolitinib and venetoclax treatment was observed in all assays, and was significantly different from the DMSO and single-dose treatments of either ruxolitinib or venetoclax in both cell lines. In addition, the synergistic effect of the dual drug delivery as compared to individual drugs (or DMSO) was observed at all but one time point (p< 0.001 for survival and p <0.0001 for proliferation **(Figure 2D)**. We next assessed both Annexin V and 7-AAD via flow cytometry and found increased Annexin V and 7-AAD in both cell lines, suggesting a synergistic benefit on viability **(Figure 2E; Supplementary Figure 2C).** The Jurkat cell line also showed a reduction of both survival for up to 5 days in culture utilizing Incucyte live-cell imaging technology (p< 0.0001 compared to no treatment) **(Figure 2C)**.

Because the combination of ruxolitinib and venetoclax was effective *in vitro* but not *in vivo*, we next assessed whether or not ruxolitinib and venetoclax were acting on their intended targets, the JAK/STAT pathway and BCL2 family, *in vitro*. When given in combination, there were decreases in total STAT1 protein by western blot analysis (**Figure 3A, B**) and pSTAT1 expression by intracellular flow cytometry (**Figure 3C**) as compared to single inhibitor and DMSO controls, while total STAT3 protein expression decreased in comparison to DMSO control (**Figure 3A**). STAT5 is not constitutively expressed in Jurkat cells, but the combination dose does lower STAT5 and pSTAT5 expression in other cell lines (data not shown). The combination dose also had an effect on several members of the BCL2 family of proteins, where the expression of the anti-apoptotic protein BCL2 decreased and the expression of pro-

apoptotic proteins, BIM and BAK, increased **(Figure 3A, B)**. These data suggest that ruxolitinib and venetoclax are acting on their intended targets *in vitro*.

Ruxolitinib and venetoclax fail to treat T-ALL *in vivo* due to leukemia CNS infiltration, and are unable to cross the BBB

Based on the robust synergistic effect of ruxolitinib and venetoclax observed *in vitro*, a xenograft model of T-ALL was established utilizing Jurkat cells and NSG mice[27,28] to test these drugs as a combination therapy *in vivo*. *In vivo* dosing was conducted to determine a synergistic dose of 30 mg/kg/day ruxolitinib and 35 mg/kg/day venetoclax delivered via oral gavage once daily[15,16,29,30] for 14- days after cancer burden establishment. Surprisingly, ruxolitinib and venetoclax failed to improve survival after T-ALL challenge when given as single agents or in combination **(Figure 4A).** We next injected NSG mice with GFP expressing Jurkat cells and analyzed the cancer burden (without ruxolitinib or venetoclax treatment) by flow cytometry for an anti-human $CD45^+GFP^+$ double population in the bone marrow, spleen, brain, and spinal cord over the course of the disease (approximately 50-60 days). Interestingly, the T-ALL burden was primarily in the spinal cord and eventually the brain, but not the bone marrow and spleen **(Figure 4B-D)**

While both inhibitors are FDA approved and currently used in the clinic, there is no published data that shows if either inhibitor has the ability to effectively penetrate the CNS. Naïve mice were treated by oral gavage with the highest published *in vivo* single dose of either ruxolitinib (50 mg/kg)[29] or venetoclax (100 mg/kg),[15] the mice were then sacrificed at the known plasma-peak concentration for each inhibitor. The peripheral blood, spinal cord, and brain were then analyzed for the presence of either inhibitor by LC-MS-MS **(Figure 3D)**. While approximately a third of the total plasma concentration of ruxolitinib was detected in the CNS,

only a small fraction of venetoclax was detected in the spinal cord, with no detection in the brain. These data show that when administered *in vivo* at dosing of 30 mg/kg/day ruxolitinib and 35 mg/kg/day venetoclax, these drugs cannot penetrate the BBB, explaining why they fail to treat CNS T-ALL disease burden in the Jurkat *in vivo* model.

T-ALL metastasizes to the CNS in part through the CXCR4-CXCL12 pathway in mice

Previously published data demonstrated that human T-ALL relapses to the CNS by exploiting the CXCR4-CXCL12 pathway.[22,24,31] Gene expression analysis of 5 pediatric T-ALL samples show CXCR4 is 1 standard deviation higher than in controls (NCI Oncogenomics pediatric tumor DB, https://pob.abcc.ncifcrf.gov/cgi-bin/JK) **(Figure 5A)**. We verified that CXCR4 protein is highly expressed on the surface of Jurkat cells via flow cytometry **(Figure 5B)**. Furthermore, using RNAScope and western blot analysis, we determined that CXCL12 mRNA and protein were expressed in the brain of NSG mice **(Figure 5C, D)**. These data suggest that mice injected with Jurkat cells could exploit the CXCR4-CXCL12 pathway, leading to CNS disease.

Using CRISPR-Cas9 technology we deleted the CXCR4 gene in Jurkat cells **(Figure 6A)**. We then injected the CXCR4-KO, or no-guide control (NGC) Jurkat cells, into mice and monitored them for clinical symptoms of T-ALL. The NGC group developed rapid symptoms of CNS disease and had to be euthanized by day 35 **(Figure 6B-D)**. Surprisingly, CXCR4-KO mice remained healthy and developed no signs of T-ALL until day 65 **(Figure 6C, D)**. The CXCR4-KO mice did not become moribund until approximately 100 days after tumor inoculation **(Figure 6A)**, 65-70 days after the NGC group succumbed to disease (p= 0.004).

Discussion:

Relapsed or refractory T-ALL remains a significant challenge to manage, especially because most patients are heavily pretreated with chemotherapy that causes significant end organ toxicity. Development of targeted therapies that inhibit pathways exploited by T-ALL to augment proliferation and survival may improve outcomes while also minimizing systemic toxicity. Prior studies involving RNA or whole genome sequencing of T-ALL samples identified the JAK/STAT pathway[32-34] and the BCL2 pathway[15] as dysregulated in these leukemias. In this study ruxolitinib, a JAK1/2 inhibitor and venetoclax, a potent BCL2 inhibitor independently decreased viability and proliferation of T-ALL *in vitro.* Further, combining these two inhibitors *in vitro*, achieved a synergistic effect demonstrating a greater increase in apoptosis and a decrease in proliferation compared to either inhibitor alone. This data confirmed findings previously demonstrated in T-ALL[20,35,36] and other cancers.[37-39]

Ruxolitinib treatment alone has been considered a breakthrough therapy for myeloproliferative neoplasms but long-term studies have shown that this treatment is not curative and does not lead to molecular or pathological remission. This may be caused by the disease evading treatment and utilizing an alternative survival pathway; such as, the BCL2 pathway. While Senkevitch et al 2018 demonstrated a robust synergistic effect of combined JAK/STAT and BCL2 inhibition *in vivo* in IL7Rα+ T-ALL, all mice succumbed to T-ALL. Our study demonstrates for the first time that T-ALL progression after combined ruxolitinib and venetoclax treatment arises from CNS invasion through CXCR4, a previous homing pathway identified in untreated T-ALL cells.[22] The xenograft model of T-ALL with Jurkat cells presents as CNS disease with the cancer burden homing primarily into the spinal cord, rather than a primary systemic form where the burden is primarily in the bone marrow, spleen, and liver.[40] This xenograft model is clinically relevant given that CNS relapse is common for T-ALL, and is a strong driver for a poor prognosis.[41]

The current standard of treating CNS leukemia is either by administering repeated doses of intrathecal chemotherapy, or giving irradiation to the neuro-axis. There is a great need to identify agents that are effective in the CNS when administered systemically. This study demonstrated for the first time that while ruxolitinib and venetoclax work synergistically *in vitro* they may be ineffective *in vivo* since they are unable to effectively cross the BBB and target CNS leukemia. LC-MS-MS demonstrated that ruxolitinib and venetoclax can be detected in the CNS, they are not at high enough concentrations to generate an anti-tumor effect at synergistic dosing. These data could be informative as future generations of these small molecule inhibitors may need to be engineered to allow for better CNS penetration.

Further we dissected the homing mechanism demonstrated with Jurkat cells in NSG mice. Several studies of human T-ALL demonstrated that CNS relapsed T-ALL occurs in part through the CXCR4-CXCL12 chemokine pathway.[22,24,25,31] We confirmed for the first time that Jurkat cells utilize this pathway to escape treatment by ruxolitinib and venetoclax and infiltrate the CNS. CXCR4 is abundantly present on the surface of Jurkat cells, and the brain of NSG mice endogenously express CXCL12 mRNA and protein. Since murine CXCL12 can bind the human CXCR4 receptor[42], human T-ALL can enter the CNS of NSG mice. Utilizing CRISPR-Cas9 to delete CXCR4 from the surface of Jurkat cells, we determined that CXCR4 plays a critical role in Jurkat cell homing to not only in the CNS but also non-CNS sites. CXCR4 deletion in T-ALL cells significantly delays lethality by 60-70 days while reducing neurological and overall clinical scores, showing that CXCR4 plays a critical role in T-ALL progression. CXCR4 has been identified as a key player in murine and human T-ALL establishment and progression.[22-24] The surface expression of CXCR4, which was demonstrated to be calcineurin dependent, is also essential to the leukemia-initiating cell (LIC) activity of T-ALL.[24] The absence of CXCR4 also results in migratory defects of T-ALL both *in vitro* and *in vivo*.[24] Furthermore, it has been demonstrated that CXCL12- producing vascular endothelial niches control the maintenance of T-ALL.[23] These niches are predominantly found in the bone marrow stroma but have also been

discovered in the brain allowing infiltration into the CNS.[22,23] Thus, inhibiting the CXCR4-CXCL12 pathway, such as with plerixafor, may be a means to prevent escape to the CNS after combination therapy with ruxolitinib and venetoclax.

Development of novel therapies for relapsed/refractory T-ALL is a high unmet need given the poor prognosis of this cancer. Inhibiting the JAK/STAT pathway along with BCL2 using ruxolitinib and venetoclax is an effective treatment for relapsed T-ALL, but requires additional inhibition of CXCR4 to prevent CNS invasion and relapse after treatment. Currently, there are no studies investigating the link between the JAK/STAT-BCL2-CXCR4 pathways. Future studies could consider targeting all 3 pathways as a means of inducing a sustained complete remission. Combination of ruxolitinib and venetoclax with cell-based therapies, like T or NK cells, could also be considered since immune effector cells can easily cross the BBB, but the impact of these drugs on these cell subsets will need to be explored carefully.

Authorship Contributions:

K.L.W. and C.M.C designed the experiments, analyzed and interpreted results and wrote the manuscript; S.A.K, F.Z., S.L.O, M.M.C., A.E.Q., A.S.F., and T.B.G. conducted experiments and analyzed data; S.A.K. and S.L.O analyzed data and generated figures; and M.N.B. and L.R. discussed and interpreted results. All authors read and approved the manuscript.

Conflicts of Interest Disclosures:

C.M.C reports honorarium from Nektar Therapeutics. This company had no input in the study design, analysis, manuscript preparation or decision to submit for publication. No other relevant conflicts of interest are reported.

References:

1.   Sanda T, Tyner JW, Gutierrez A, et al. TYK2-STAT1-BCL2 pathway dependence in T-cell acute lymphoblastic leukemia. *Cancer Discov*. 2013;3(5):564-577.

2.   Follini E, Marchesini M, Roti G. Strategies to Overcome Resistance Mechanisms in T-Cell Acute Lymphoblastic Leukemia. *Int J Mol Sci*. 2019;20(12).

3.   Marks DI, Rowntree C. Management of adults with T-cell lymphoblastic leukemia. *Blood*. 2017;129(9):1134-1142.

4.   Asselin BL, Devidas M, Wang C, et al. Effectiveness of high-dose methotrexate in T-cell lymphoblastic leukemia and advanced-stage lymphoblastic lymphoma: a randomized study by the Children's Oncology Group (POG 9404). *Blood*. 2011;118(4):874-883.

5.   Van Vlierberghe P, Ferrando A. The molecular basis of T cell acute lymphoblastic leukemia. *J Clin Invest*. 2012;122(10):3398-3406.

6.   Goldberg JM, Silverman LB, Levy DE, et al. Childhood T-cell acute lymphoblastic leukemia: the Dana-Farber Cancer Institute acute lymphoblastic leukemia consortium experience. *J Clin Oncol*. 2003;21(19):3616-3622.

7.   Marks DI, Paietta EM, Moorman AV, et al. T-cell acute lymphoblastic leukemia in adults: clinical features, immunophenotype, cytogenetics, and outcome from the large randomized prospective trial (UKALL XII/ECOG 2993). *Blood*. 2009;114(25):5136-5145.

8.   Kucine N, Marubayashi S, Bhagwat N, et al. Tumor-specific HSP90 inhibition as a therapeutic approach in JAK-mutant acute lymphoblastic leukemias. *Blood*. 2015;126(22):2479-2483.

9.   Delgado-Martin C, Meyer LK, Huang BJ, et al. JAK/STAT pathway inhibition overcomes IL7-induced glucocorticoid resistance in a subset of human T-cell acute lymphoblastic leukemias. *Leukemia*. 2017;31(12):2568-2576.

10.   Liszewski W, Naym DG, Biskup E, Gniadecki R. Psoralen with ultraviolet A-induced apoptosis of cutaneous lymphoma cell lines is augmented by type I interferons via the JAK1-STAT1 pathway. *Photodermatol Photoimmunol Photomed*. 2017;33(3):164-171.

11.   Senkevitch E, Durum S. The promise of Janus kinase inhibitors in the treatment of hematological malignancies. *Cytokine*. 2017;98:33-41.

12.   Messina NL, Banks KM, Vidacs E, et al. Modulation of antitumour immune responses by intratumoural Stat1 expression. *Immunol Cell Biol*. 2013;91(9):556-567.

13.   Seymour JF, Kipps TJ, Eichhorst B, et al. Venetoclax-Rituximab in Relapsed or Refractory Chronic Lymphocytic Leukemia. *N Engl J Med*. 2018;378(12):1107-1120.

14.   Seymour JF, Mobasher M, Kater AP. Venetoclax-Rituximab in Chronic Lymphocytic Leukemia. *N Engl J Med*. 2018;378(22):2143-2144.

15.   Chonghaile TN, Roderick JE, Glenfield C, et al. Maturation stage of T-cell acute lymphoblastic leukemia determines BCL-2 versus BCL-XL dependence and sensitivity to ABT-199. *Cancer Discov*. 2014;4(9):1074-1087.

16.   Peirs S, Matthijssens F, Goossens S, et al. ABT-199 mediated inhibition of BCL-2 as a novel therapeutic strategy in T-cell acute lymphoblastic leukemia. *Blood*. 2014;124(25):3738-3747.

17.   Koppikar P, Bhagwat N, Kilpivaara O, et al. Heterodimeric JAK-STAT activation as a mechanism of persistence to JAK2 inhibitor therapy. *Nature*. 2012;489(7414):155-159.

18.   Matulis SM, Gupta VA, Nooka AK, et al. Dexamethasone treatment promotes Bcl-2 dependence in multiple myeloma resulting in sensitivity to venetoclax. *Leukemia*. 2016;30(5):1086-1093.

19.   Zhang M, Mathews Griner LA, Ju W, et al. Selective targeting of JAK/STAT signaling is potentiated by Bcl-xL blockade in IL-2-dependent adult T-cell leukemia. *Proc Natl Acad Sci U S A*. 2015;112(40):12480-12485.

20.   Senkevitch E, Li W, Hixon JA, et al. Inhibiting Janus Kinase 1 and BCL-2 to treat T cell acute lymphoblastic leukemia with IL7-Ralpha mutations. *Oncotarget*. 2018;9(32):22605-22617.

21.   Pui CH, Robison LL, Look AT. Acute lymphoblastic leukaemia. *Lancet*. 2008;371(9617):1030-1043.

22.   T RJ. Role of CXCR4-mediated bone marrow colonization in CNS infiltration by T cell acute lymphoblastic leukemia. *Journal of Leukocyte Biology*. 2016;99:1077-1087.

23.   Pitt LA, Tikhonova AN, Hu H, et al. CXCL12-Producing Vascular Endothelial Niches Control Acute T Cell Leukemia Maintenance. *Cancer Cell*. 2015;27(6):755-768.

24.   Passaro D, Irigoyen M, Catherinet C, et al. CXCR4 Is Required for Leukemia-Initiating Cell Activity in T Cell Acute Lymphoblastic Leukemia. *Cancer Cell*. 2015;27(6):769-779.

25.   Yao H, Price TT, Cantelli G, et al. Leukaemia hijacks a neural mechanism to invade the central nervous system. *Nature*. 2018;560(7716):55-60.

26.   Anderson NM, Harrold I, Mansour MR, et al. BCL2-specific inhibitor ABT-199 synergizes strongly with cytarabine against the early immature LOUCY cell line but not more-differentiated T-ALL cell lines. *Leukemia*. 2014;28(5):1145-1148.

27.   Maude SL, Tasian SK, Vincent T, et al. Targeting JAK1/2 and mTOR in murine xenograft models of Ph-like acute lymphoblastic leukemia. *Blood*. 2012;120(17):3510-3518.

28.   Wu X, Zhang LS, Toombs J, et al. Extra-mitochondrial prosurvival BCL-2 proteins regulate gene transcription by inhibiting the SUFU tumour suppressor. *Nat Cell Biol*. 2017;19(10):1226-1236.

29.   Carniti C, Gimondi S, Vendramin A, et al. Pharmacologic Inhibition of JAK1/JAK2 Signaling Reduces Experimental Murine Acute GVHD While Preserving GVT Effects. *Clin Cancer Res*. 2015;21(16):3740-3749.

30.   Khaw SL, Suryani S, Evans K, et al. Venetoclax responses of pediatric ALL xenografts reveal sensitivity of MLL-rearranged leukemia. *Blood*. 2016;128(10):1382-1395.

31.   Burger JA, Peled A. CXCR4 antagonists: targeting the microenvironment in leukemia and other cancers. *Leukemia*. 2009;23(1):43-52.

32.   Zhang J, Ding L, Holmfeldt L, et al. The genetic basis of early T-cell precursor acute lymphoblastic leukaemia. *Nature*. 2012;481(7380):157-163.

33.   Gianfelici V, Chiaretti S, Demeyer S, et al. RNA sequencing unravels the genetics of refractory/relapsed T-cell acute lymphoblastic leukemia. Prognostic and therapeutic implications. *Haematologica*. 2016;101(8):941-950.

34.   Liu Y, Easton J, Shao Y, et al. The genomic landscape of pediatric and young adult T-lineage acute lymphoblastic leukemia. *Nat Genet*. 2017;49(8):1211-1218.

35.   Degryse S, de Bock CE, Demeyer S, et al. Mutant JAK3 phosphoproteomic profiling predicts synergism between JAK3 inhibitors and MEK/BCL2 inhibitors for the treatment of T-cell acute lymphoblastic leukemia. *Leukemia*. 2018;32(3):788-800.

36.   Kontro M, Kuusanmaki H, Eldfors S, et al. Novel activating STAT5B mutations as putative drivers of T-cell acute lymphoblastic leukemia. *Leukemia*. 2014;28(8):1738-1742.

37.   Karjalainen R, Pemovska T, Popa M, et al. JAK1/2 and BCL2 inhibitors synergize to counteract bone marrow stromal cell-induced protection of AML. *Blood*. 2017;130(6):789-802.

38.   Kuusanmaki H, Leppa AM, Polonen P, et al. Phenotype-based drug screening reveals association between venetoclax response and differentiation stage in acute myeloid leukemia. *Haematologica*. 2019.

39.   Waibel M, Solomon VS, Knight DA, et al. Combined targeting of JAK2 and Bcl-2/Bcl-xL to cure mutant JAK2-driven malignancies and overcome acquired resistance to JAK2 inhibitors. *Cell Rep*. 2013;5(4):1047-1059.

40.   Vadillo E, Dorantes-Acosta E, Pelayo R, Schnoor M. T cell acute lymphoblastic leukemia (T-ALL): New insights into the cellular origins and infiltration mechanisms common and unique among hematologic malignancies. *Blood Rev.* 2018;32(1):36-51.

41.   Nguyen K, Devidas M, Cheng SC, et al. Factors influencing survival after relapse from acute lymphoblastic leukemia: a Children's Oncology Group study. *Leukemia.* 2008;22(12):2142-2150.

42.   Beider K, Nagler A, Wald O, et al. Involvement of CXCR4 and IL-2 in the homing and retention of human NK and NK T cells to the bone marrow and spleen of NOD/SCID mice. *Blood.* 2003;102(6):1951-1958.

Figure Legends:

Figure 1. The JAK/STAT and BCL2 pathway is dysregulated in patient samples of T-ALL; Jurkat T-ALL can be targeted by ruxolitinib and venetoclax (A) JAK/STAT and BCL2 gene expression data of 14 different T-ALL patient samples. https://pob.abcc.ncifcrf.gov/cgi-bin/JK St. Jude Affy U133AB DB (B) Trypan blue exclusion data of serial diluted ruxolitinib at 24, 48 and 72 h (C) Trypan blue exclusion data of serial diluted venetoclax at 24, 48, 72 h (D) MTT proliferation data of serial diluted ruxolitinib at 24, 48, and 72 h (E) MTT proliferation data of serial diluted venetoclax at 24, 48, 72 h. Experiments were duplicated with (n =3) each experiment.

Figure 2. Ruxolitinib and venetoclax synergistically decrease survival and proliferation of jurkat cells (A) Trypan blue exclusion data of combination treatment and single dose controls (B) MTT proliferation data of combination treatment and single dose controls (C) Incucyte *in vitro* live cell imaging of combination treatment over the course of 5 days. Cell death was quantified by lack of GFP expression (D) Compusyn data determining that ruxolitinib and venetoclax work in a synergistic manner (http://www.combosyn.com/) (E) Annexin V and & 7-AAD data of combination treatment and single dose controls after 48 h treatment. Experiments were duplicated with (n =3) each experiment.

Figure 3. Target analysis of ruxolitinib and venetoclax (A) Western blot analysis of JAK/STAT and BCL2 proteins in Jurkat cells treated with vehicle control, ruxolitinib, venetoclax or combination for 24h. (B) Statistical representation of the fold change of protein density normalized to positive control compared to DMSO control (C) Flow analysis of pSTAT1 and pSTAT3 (D) LC-MS-MS of naïve NSG mice after oral gavage treatment of either 50 mg/kg of ruxolitinib or 100 mg/kg venetoclax (n =3).

Figure 4. Ruxolitinib and venetoclax combination does not affect cancer burden *in vivo*; T-ALL accumulates in the CNS (A) Survival curve of vehicle control, 30mg/kg ruxolitinib, 35mg/kg venetoclax, and combination *in vivo* (n =5). (B) Day 50 immunohistochemistry of spleen and brain sections stained with DAPI and rabbit anti-GFP primary and a goat anti-rabbit Alexa Fluor 555 secondary antibody of NSG mice injected with Jurkat-GFP cells. (C) Time course between Day 0-50 of Jurkat-GFP and anti-human CD45 cancer burden in bone marrow, brain, liver, and spinal cord (n =3) (D) Statistical representation of percent GFP,CD45, cancer burden in bone marrow, brain, liver, and spinal cord.

Figure 5. CXCR4 expression on Jurkat cells and CXCL12 expression in the NSG brain (A) CXCR4 gene expression data of 5 pediatric tumor samples. https://pob.abcc.ncifcrf.gov/cgi-bin/JK pediatric tumor DB (B) Jurkat cells were analyzed by FACS analysis for the presence of surface CXCR4. The red line represents staining with CXCR4 antibody and the blue line represents FMO control. (C) CXCL12 mRNA expression in the NSG brain was analyzed using RNAScope analysis (n =3). (D) CXCL12 protein expression in the NSG brain was analyzed by western blot analysis (n =3). Whole mouse CXCL12 protein generated in *E.coli* was used as a positive control.

Figure 6.CXCR4 knock-out effects *in vivo* engraftment (A) CXCR4 knock-out success was confirmed by flow analysis compared to the no guide control (B) Survival analysis of NSG mice injected with either CXCR4-KO cells or NGC cells (n =3) (C) Total clinical score analysis of CXCR4-KO group compared to NGC group (D) CNS clinical score analysis of CXCR4-KO group compared to NGC group.
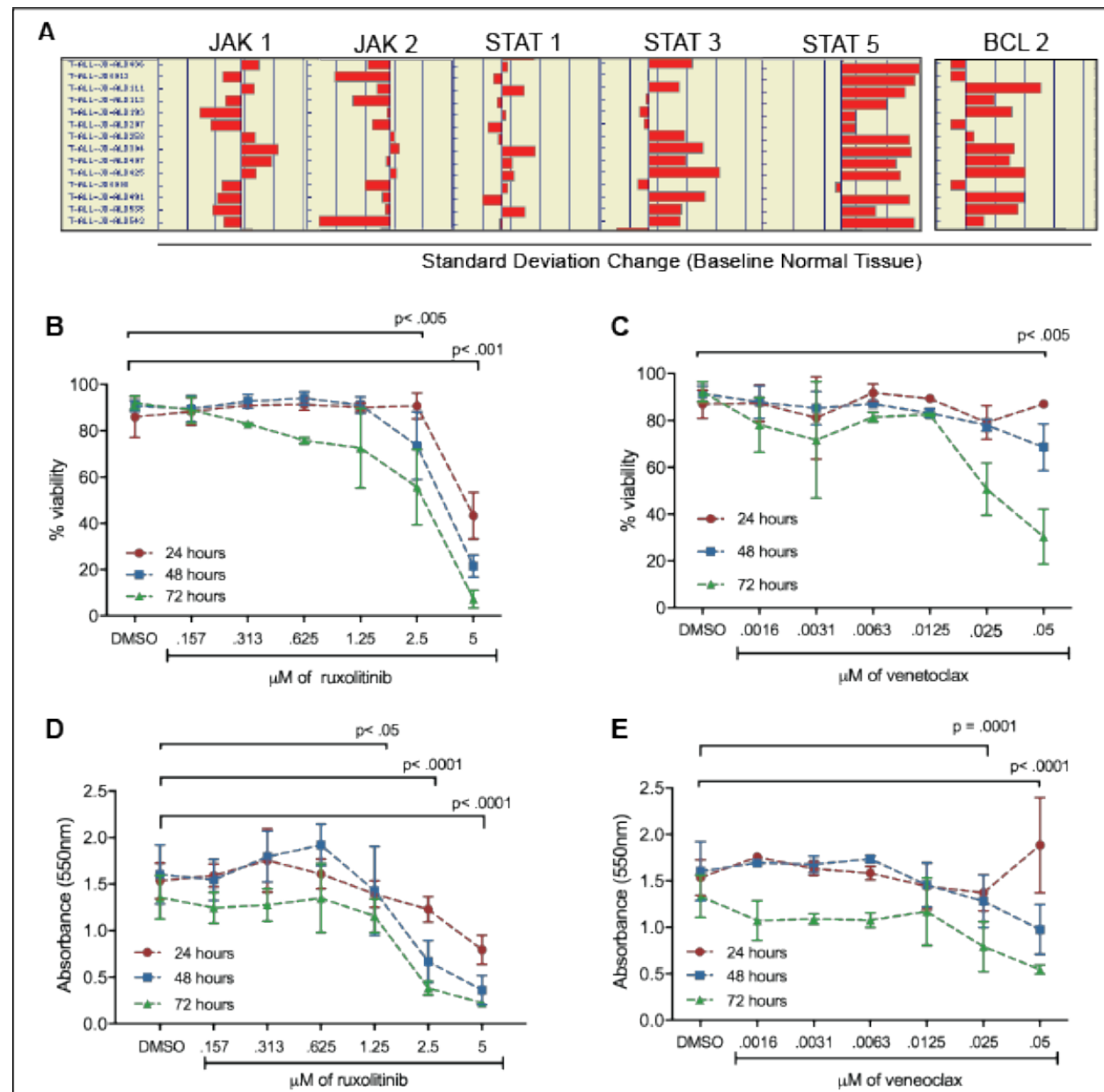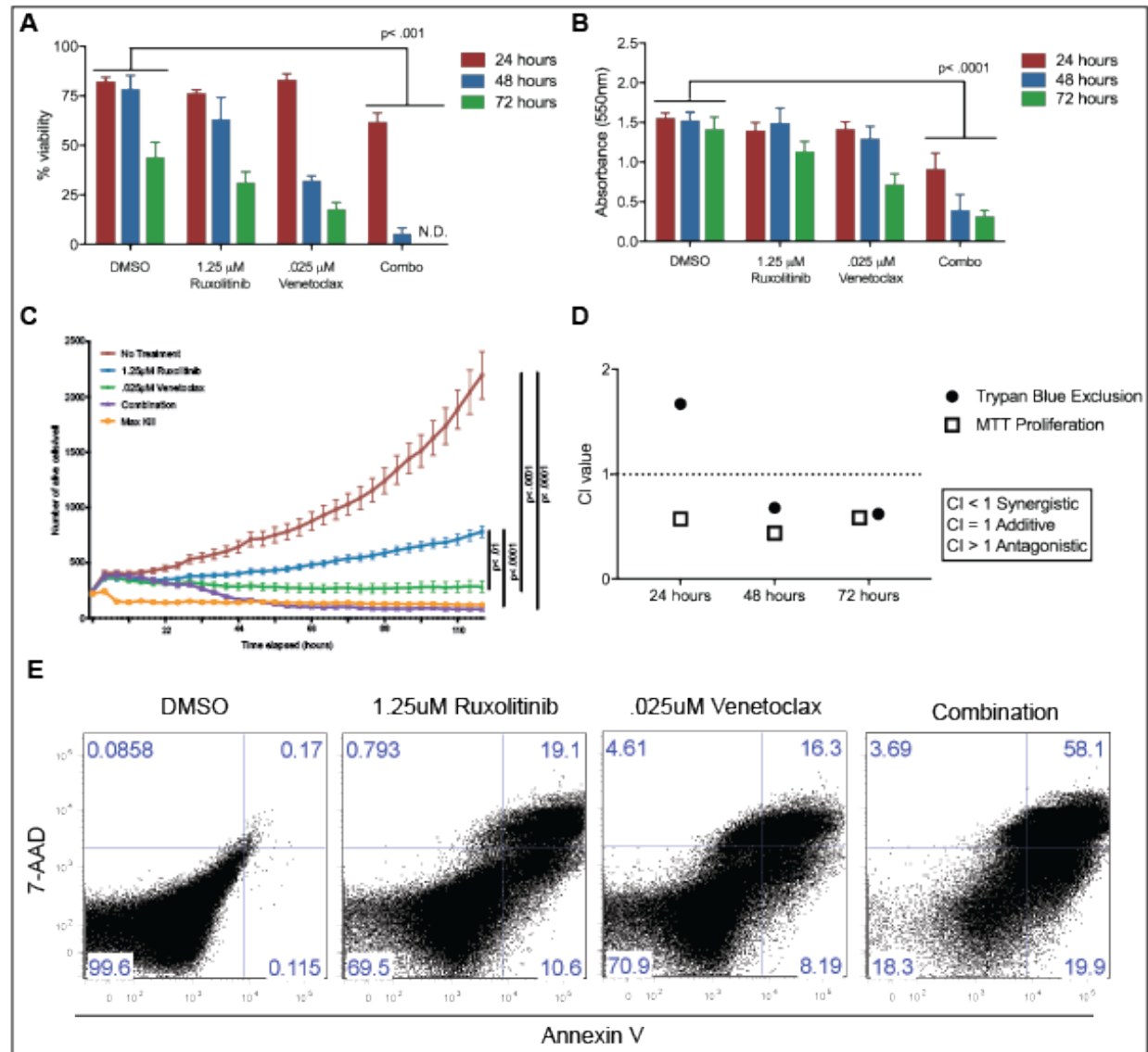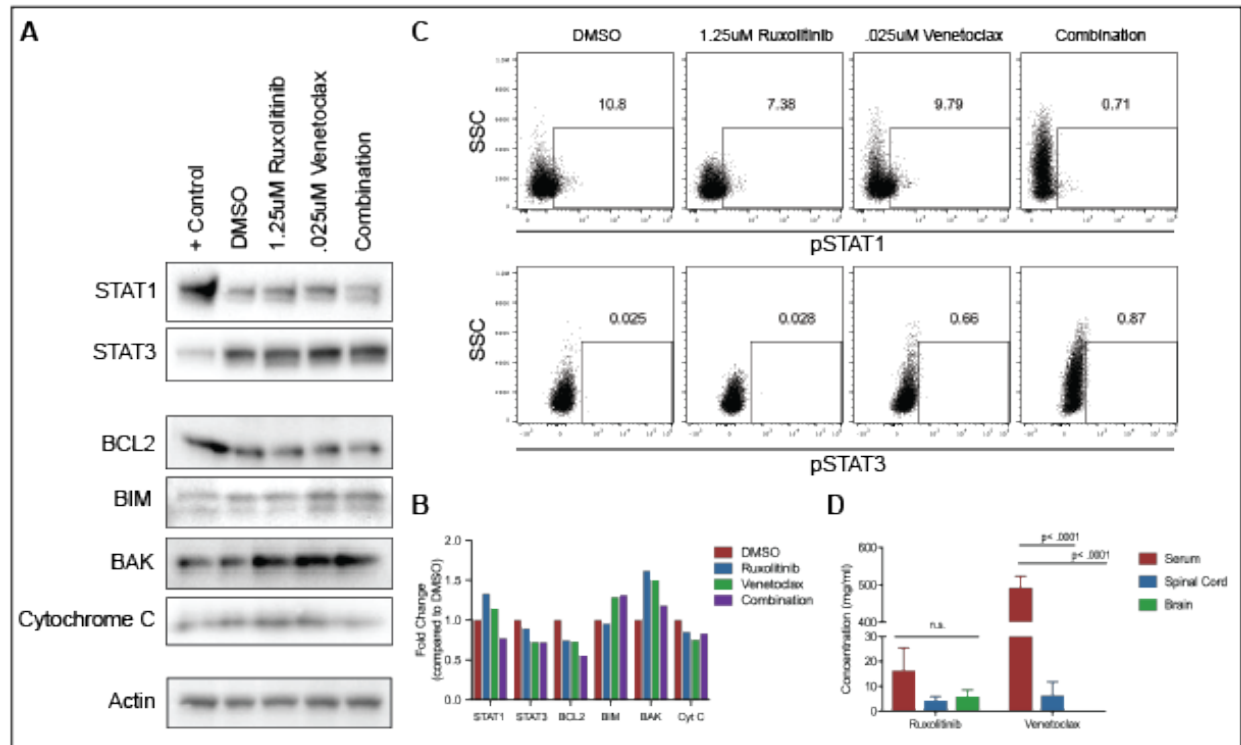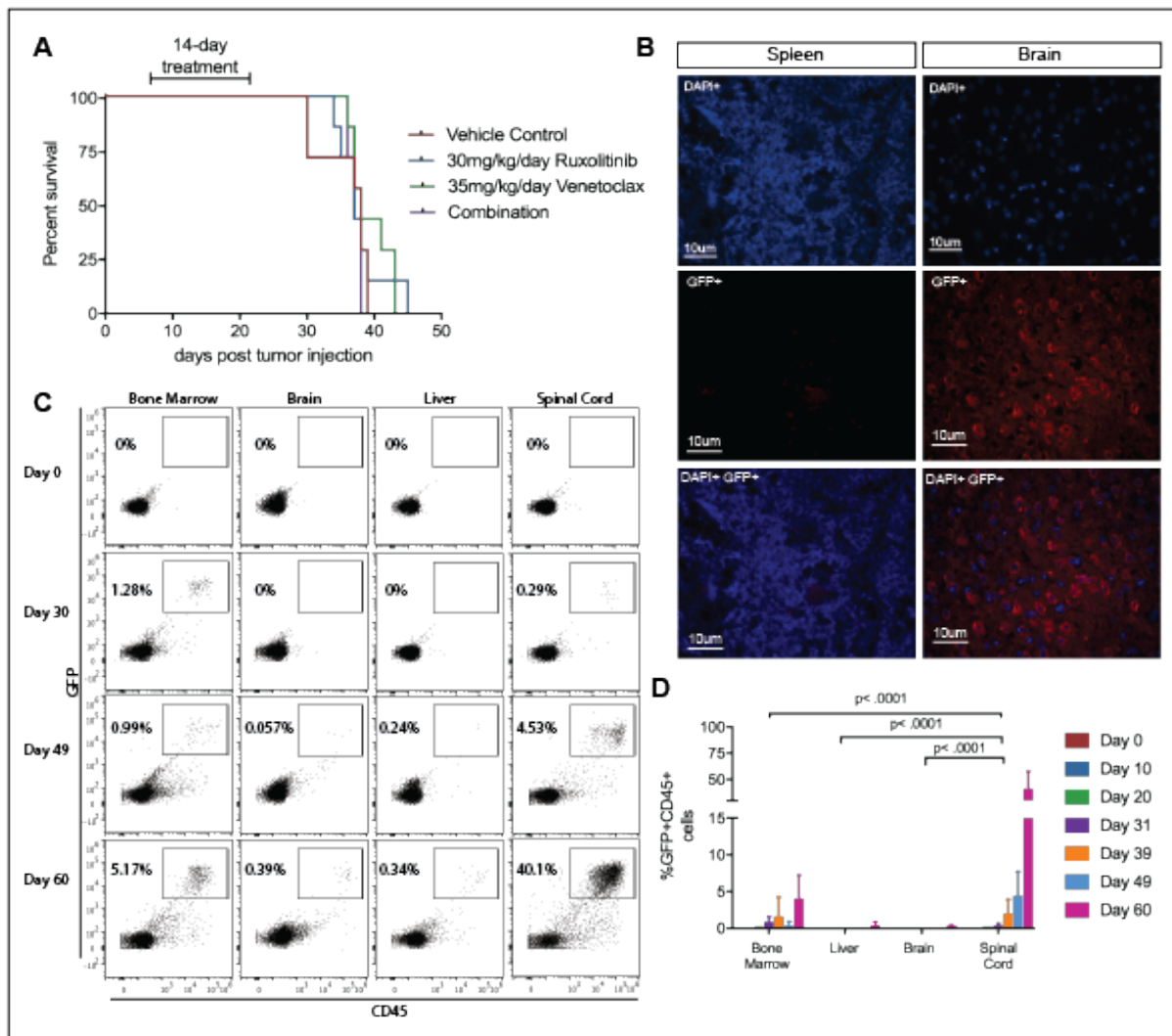
Figure 1

Figure 2

Figure 3

Figure 4

Figure 5

Figure 6